

# Probabilistic Permutation Synchronization using the Riemannian Structure of the Birkhoff Polytope

Tolga Birdal<sup>1,2</sup> Umut Şimşekli<sup>3</sup>

<sup>1</sup> Computer Science Department, Stanford University, CA 94305 Stanford, US

<sup>2</sup> Fakultät für Informatik, Technische Universität München, 85748 München, Germany

<sup>3</sup> LTCI, Télécom ParisTech, Université Paris-Saclay, 75013 Paris, France

## Abstract

We present an entirely new geometric and probabilistic approach to synchronization of correspondences across multiple sets of objects or images. In particular, we present two algorithms: (1) Birkhoff-Riemannian L-BFGS for optimizing the relaxed version of the combinatorially intractable cycle consistency loss in a principled manner; (2) Birkhoff-Riemannian Langevin Monte Carlo for generating samples on the Birkhoff Polytope and estimating the confidence of the found solutions. To this end, we first introduce the very recently developed Riemannian geometry of the Birkhoff Polytope. Next, we introduce a new probabilistic synchronization model in the form of a Markov Random Field (MRF). Finally, based on the first order retraction operators, we formulate our problem as simulating a stochastic differential equation and devise new integrators. We show on both synthetic and real datasets that we achieve high quality multi-graph matching results with faster convergence and reliable confidence/uncertainty estimates.

## 1. Introduction

Correspondences fuel a large variety of computer vision applications such as structure-from-motion (SfM) [62], SLAM [53], 3D reconstruction [20, 8, 6], camera re-localization [60], image retrieval [44] and 3D scan stitching [38, 22]. In a typical scenario, given two scenes, an initial set of 2D/3D keypoints is first identified. Then the neighborhood of each keypoint is summarized with a local descriptor [47, 23] and keypoints in the given scenes are matched by associating the mutually closest descriptors. In a majority of practical applications, multiple images or 3D shapes are under consideration and ascertaining such two-view or *pairwise* correspondences is simply not sufficient. This necessitates a further refinement ensuring global consistency. Unfortunately, at this stage even the well developed pipelines acquiesce either heuristic/greedy refinement [21] or incorporate costly geometric cues related to the linking of individual correspondence estimates into a

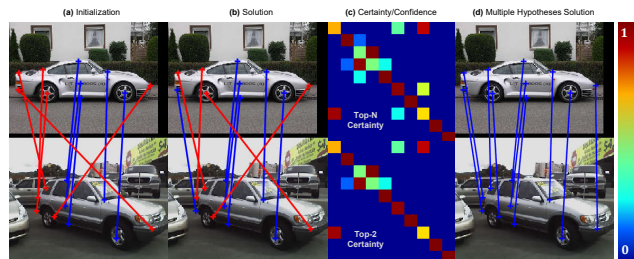


Figure 1. Our algorithm robustly solves the multiway image matching problem (a, b) and provides confidence maps (c) that can be of great help in further improving the estimates (d). The bar on the right is used to assign colors to confidences. For the rest, incorrect matches are marked in red and correct ones in blue.

globally coherent whole [30, 62, 73].

In this paper, by using the fact that correspondences are *cycle consistent*<sup>1</sup>, we propose two novel algorithms for refining the assignments across multiple images/scans (nodes) in a *multi-way graph* and for estimating assignment confidences, respectively. We model the correspondences between image pairs as *relative, total* permutation matrices and seek to find *absolute* permutations that re-arrange the detected keypoints to a single canonical, global order. This problem is known as *map* or *permutation synchronization* [56, 70]. Even though in many practical scenarios matches are only partially available, when shapes are complete and the density of matches increases, total permutations can suffice [36].

Similar to many well received works [84, 61], we relax the sought permutations to the set of doubly-stochastic (DS) matrices. We then consider the geometric structure of DS, the *Birkhoff Polytope* [9]. We are - to the best of our knowledge, for the first time introducing and applying the recently developed Riemannian geometry of the Birkhoff Polytope [26] to tackle challenging problems of computer vision. Note that lack of this geometric understanding caused plenty of obstacles for scholars dealing with our problem [61, 77]. By the virtue of a first order retraction, we

<sup>1</sup>Composition of correspondences for any circular path arrives back at the start node.

can use the recent Riemannian limited-memory BFGS (LR-BFGS) algorithm [82] to perform a maximum-a-posteriori (MAP) estimation of the parameters of the consistency loss. We coin our variation as *Birkhoff-LRBFGS*.

At the next stage, we take on the challenge of confidence/uncertainty estimation for the problem at hand by drawing samples on the Birkhoff Polytope and estimating the empirical posterior distribution. To achieve this, we first formulate a new geodesic stochastic differential equation (SDE). Our SDE is based upon the Riemannian Langevin Monte Carlo (RLMC) [31, 78, 58] that is efficient and effective in sampling from Riemannian manifolds with *true* exponential maps. Note that similar stochastic gradient geodesic MCMC (SG-MCMC) [46, 11] tools have already been used in the context of synchronization of spatial rigid transformations whose parameters admit an analytically defined geodesic flow [7]. Unfortunately, for our manifold the retraction map is only up to first order and hence we cannot use off-the-shelf schemes. Alleviating this nuisance, we further contribute a novel numerical integrator to solve our SDE by replacing the intractable exponential map of DS matrices by the approximate retraction map. This leads to another new algorithm: *Birkhoff-RLMC*.

In a nutshell, our contributions are:

1. We function as an ambassador and introduce the Riemannian geometry of the Birkhoff Polytope [26] to solve problems in computer vision.
2. We propose a new probabilistic model for the permutation synchronization problem.
3. We minimize the cycle consistency loss via a Riemannian-LBFGS algorithm and outperform the state-of-the-art both in recall and in runtime.
4. Based upon the Langevin mechanics, we introduce a new SDE and a numerical integrator to draw samples on the high dimensional and complex manifolds with approximate retractions, such as the Birkhoff Polytope. This lets us estimate the confidence maps, which can aid in improving the solutions and spotting consistency violations or outliers.

Note that the tools developed herewith can easily extend beyond our application and would hopefully facilitate promising research directions regarding the combinatorial optimization problems in computer vision.

## 2. Related Work

Permutation synchronization is an emerging domain of study due to its wide applicability, especially for the problems in computer vision. We now review the developments in this field, as chronologically as possible. Note that multi-way graph matching problem formulations involving spatial geometry are well studied [18, 50, 43, 29, 79, 19], as well as transformation synchronization [76, 13, 72, 75, 3, 4, 33]. For brevity, we omit these literature and focus on works that explicitly operate on correspondence matrices.

The first applications of *synchronization*, a term coined by Singer [67, 66], to correspondences only date back to early 2010s [54]. Pachauri *et al.* [56] gave a formal definition and devised a spectral technique. The same authors quickly extended their work to Permutation Diffusion Maps [55] finding correspondence between images. Unfortunately, this first method was quadratic in the number of images and hence was not computationally friendly. In a sequel of works called *MatchLift*, Huang, Chen and Guibas [36, 15] were the firsts to cast the problem of estimating cycle-consistent maps as finding the closest positive semidefinite matrix to an input matrix. They also addressed the case of partial permutations. Due to the semidefinite programming (SDP) involved, this perspective suffered from high computational cost in real applications. Similar to Pachauri [56], for  $N$  images and  $M$  edges, this method required computing an eigendecomposition of an  $NM \times NM$  matrix. Zhou *et al.* [85] then introduced *MatchALS*, a new low-rank formulation with nuclear-norm relaxation, globally solving the joint matching of a set of images without the need of SDP. Yu *et al.* [81] formulated a synchronization energy similar to our method and proposed proximal Gauss-Seidel methods for solving a relaxed problem. However, unlike us, this paper did not use the geometry of the constraints or variables and thereby resorted to complicated optimization procedures involving Frank-Wolfe subproblems for global constraint satisfaction. Arrigoni *et al.* [2] and Maset *et al.* [2] extended Pachauri [56] to operate on partial permutations using spectral decomposition. To do so, they considered the symmetric inverse semigroup of the partial matches that are typically hard to handle. Their closed form methods did not need initialization steps to synchronize, but also did not establish an explicit cycle consistency. Tang *et al.* [71] opted to use ordering heuristics improving upon Pachauri [56]. Cosmo *et al.* [19] brought an interesting solution to the problem of estimating consistent correspondences between multiple 3D shapes, without requiring initial pairwise solutions as input. Schiavinato and Torsello [61] tried to overcome the lack of group structure of the Birkhoff polytope by transforming any graph-matching problem into a multi-graph matching one. Bernard *et al.* [5] used an NMF-based approach to generate a cycle-consistent synchronization. Park and Yoon [57] used multi-layer random walks framework to address the global correspondence search problem of multi-attributed graphs. Starting from a multi-layer random-walks initialization, the authors proposed a robust solver by iterative reweighting. Hu *et al.* [35] revisited the *MatchLift* and developed a scalable, distributed solution with the help of ADMMs, called *DMatch*. Their idea of splitting the input into sub-collections can still lead to global consistency under mild conditions while improving the efficiency. Finally, Wang *et al.* [77] made use of the domain knowledge and added the geometric consistency of image coordinates as a

low-rank term to increase the recall.

The aforementioned works have neither considered the Riemannian structure of the common Birkhoff convex relaxation nor have they provided a probabilistic framework, which can pave the way to uncertainty estimation while simultaneously solving the optimization problem. This is what we propose in this work.

### 3. Preliminaries and Technical Background

**Definition 1** (Permutation Matrix). *A permutation matrix is defined as a sparse, square binary matrix, where each column and each row contains only a single true (1) value:*

$$\mathcal{P}_n := \{\mathbf{P} \in \{0,1\}^{n \times n} : \mathbf{P}\mathbf{1}_n = \mathbf{1}_n, \mathbf{1}_n^\top \mathbf{P} = \mathbf{1}_n^\top\}. \quad (1)$$

where  $\mathbf{1}_n$  denotes a  $n$ -dimensional ones vector. Every  $\mathbf{P} \in \mathcal{P}^n$  is a total permutation matrix and  $P_{ij} = 1$  implies that element  $i$  is mapped to element  $j$ . Permutation matrices are the only strictly non-negative elements of the orthogonal group  $\mathcal{P}_n \in \mathcal{O}_n = \{\mathbf{O} : \mathbf{O}^\top \mathbf{O} = \mathbf{I}\}$ , a special case of the Stiefel manifold of  $m$ -frames in  $\mathbb{R}_n$  when  $m = n$ .

**Definition 2** (Center of Mass). *The center of mass for all the permutations on  $n$  objects is defined in  $\mathbb{R}^{n \times n}$  as [59]:*

$$\mathbf{C}_n = \frac{1}{n!} \sum_{\mathbf{P}_i \in \mathcal{P}_n} \mathbf{P}_i = \frac{1}{n!} (n-1)! \mathbf{1}_n \mathbf{1}_n^\top = \frac{1}{n} \mathbf{1}_n \mathbf{1}_n^\top. \quad (2)$$

Notice that  $\mathbf{C}_n \notin \mathcal{P}^n$  as shown in Fig. 2.

**Definition 3** (Relative Permutation). *We define a permutation matrix to be **relative** if it is the ratio (or difference) of two group elements ( $i \rightarrow j$ ):  $\mathbf{P}_{ij} = \mathbf{P}_i \mathbf{P}_j^\top$ .*

**Definition 4** (Permutation Synchronization Problem). *Given a redundant set of measures of ratios  $\{\mathbf{P}_{ij}\} : (i,j) \in \mathcal{E} \subset \{1, \dots, N\} \times \{1, \dots, N\}$ , where  $\mathcal{E}$  denotes the set of the edges of a directed graph of  $N$  nodes, the permutation synchronization [56] can be formulated as the problem of recovering  $\{\mathbf{P}_i\}$  for  $i = 1, \dots, N$  such that the group consistency constraint is satisfied:  $\mathbf{P}_{ij} = \mathbf{P}_i \mathbf{P}_j^{-1}$ .*

If the input data is noise-corrupted, this consistency will not hold and to recover the *absolute permutations*  $\{\mathbf{P}_i\}$ , some form of a *consistency error* is minimized. Typically, any form of minimization on the discrete space of permutations is intractable and these matrices are relaxed by their doubly-stochastic counterparts [10, 84, 61] (see Fig. 2).

**Definition 5** (Doubly Stochastic (DS) Matrix). *A DS matrix is a non-negative, square matrix whose rows and columns sum to 1. The set of DS matrices is defined as:*

$$\mathcal{DP}_n = \left\{ \mathbf{X} \in \mathbb{R}_+^{n \times n} : \sum_{i=1}^n x_{ij} = 1 \wedge \sum_{j=1}^n x_{ij} = 1 \right\}. \quad (3)$$

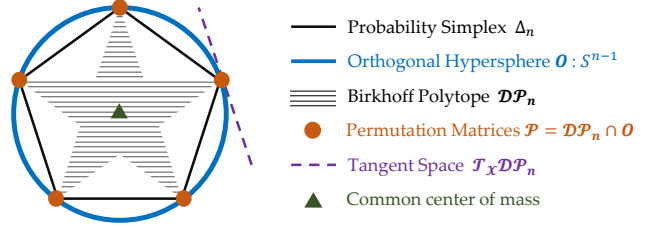


Figure 2. Simplified (matrices are vectorized) illustration of geometries we consider: (i)  $\Delta_n$  is convex, (ii)  $\mathcal{DP}_n$  is strictly contained in  $\Delta_n$ . In low dimensions, such configuration cannot exist as there is no convex shape that touches  $\Delta_n$  only on the corners.

**Theorem 1** (Birkhoff-von Neumann Theorem). *The convex hull of the set of all permutation matrices is the set of doubly-stochastic matrices and there exists a potentially non-unique  $\theta$  such that any DS matrix can be expressed as a linear combination of  $k$  permutation matrices [9, 39]:*

$$\mathbf{X} = \theta_1 \mathbf{P}_1 + \dots + \theta_k \mathbf{P}_k, \theta_i > 0 \wedge \theta^\top \mathbf{1}_k = 1. \quad (4)$$

While finding the minimum  $k$  is shown to be NP-hard [27], by Marcus-Ree theorem, we know that there exists one constructible decomposition where  $k < (n-1)^2 + 1$ .

**Definition 6** (Birkhoff Polytope). *The multinomial manifold of DS matrices is incident to the convex object called the Birkhoff Polytope [9], an  $(n-1)^2$  dimensional convex submanifold of the ambient  $\mathbb{R}^{n \times n}$  with  $n!$  vertices:  $\mathcal{B}_n \equiv \mathcal{DP}_n$ . We use  $\mathcal{DP}_n$  to refer to the Birkhoff Polytope.*

It is interesting to see that this convex polytope is co-centered with  $\mathcal{P}_n$  at  $\mathbf{C}_n$ ,  $\mathbf{C}_n \in \mathcal{DP}_n$  and over-parameterizes the convex hull of the permutation vectors, the *permutahedron* [32].  $\mathcal{P}_n$  can now be considered as an orthogonal subset of  $\mathcal{DP}_n$ :  $\mathcal{P}_n = \{\mathbf{X} \in \mathcal{DP}_n : \mathbf{X}\mathbf{X}^\top = \mathbf{I}\}$ , i.e. the discrete set of permutation matrices is the intersection of the convex set of DS matrices and the  $\mathcal{O}_n$ .

#### 3.1. Riemannian Geometry of the Birkhoff Polytope

Recently, Douik *et al.* [26] endowed  $\mathcal{DP}_n$  with the Fisher information metric, resulting in the Riemannian manifold of  $\mathcal{DP}_n$ . To the best of our knowledge, we are the first to exploit this manifold in the domain of computer vision, and hence will now recall the main results of Douik *et al.* [26] and summarize the main constructs of Riemannian optimization on  $\mathcal{DP}_n$ . The proofs can be found in [26].

**Definition 7** (Tangent Space and Bundle). *The tangent bundle is referred to as the union of all tangent spaces  $T\mathcal{DP}_n = \cup_{\mathbf{X} \in \mathcal{DP}_n} T_{\mathbf{X}}\mathcal{DP}_n$  one of which is defined as:*

$$T_{\mathbf{X}}\mathcal{DP}_n := \{\mathbf{Z} \in \mathbb{R}^{n \times n} : \mathbf{Z}\mathbf{1}_n = \mathbf{0}_n, \mathbf{Z}^\top \mathbf{1}_n = \mathbf{0}_n\}. \quad (5)$$

**Theorem 2.** *The projection operator  $\Pi_{\mathbf{X}}(\mathbf{Y})$ ,  $\mathbf{Y} \in \mathcal{DP}_n$  onto the tangent space of  $\mathbf{X} \in \mathcal{DP}_n$ ,  $T_{\mathbf{X}}\mathcal{DP}_n$  is written as:*

$$\Pi_{\mathbf{X}}(\mathbf{Y}) = \mathbf{Y} - (\alpha \mathbf{1}^\top + \mathbf{1} \beta^\top) \odot \mathbf{X}, \quad \text{with} \quad (6)$$

$$\alpha = (\mathbf{I} - \mathbf{X}\mathbf{X}^\top)^+(\mathbf{Y} - \mathbf{X}\mathbf{Y}^\top)\mathbf{1}, \quad \beta = \mathbf{Y}^\top\mathbf{1} - \mathbf{X}^\top\alpha,$$

$+$  depicts the left pseudo-inverse and  $\odot$  the Hadamard product. Note that there exists a numerically more stable way to compute the same concise formulation of  $\Pi_{\mathbf{X}}(\mathbf{Y})$  [26].

**Theorem 3.** For a vector  $\xi_{\mathbf{X}} \in \mathcal{T}_{\mathbf{X}}\mathcal{DP}_n$  lying on the tangent space of  $\mathbf{X} \in \mathcal{DP}_n$ , the first order retraction map  $R_{\mathbf{X}}$  is given as follows:

$$R_{\mathbf{X}}(\xi_{\mathbf{X}}) = \Pi(\mathbf{X} \odot \exp(\xi_{\mathbf{X}} \oslash \mathbf{X})), \quad (7)$$

where the operator  $\Pi$  denotes the projection onto  $\mathcal{DP}_n$ , efficiently computed using the Sinkhorn algorithm [68] and  $\oslash$  is the Hadamard division.

Plis *et al.* [59] showed that on the  $n$ -dimensional Birkhoff Polytope all permutations are equidistant from the center of mass  $\mathbf{C}_n$ , and thus the extreme points of  $\mathcal{DP}_n$ , that are the permutation matrices, are located on an  $(n-1)^2$ -dimensional hypersphere  $S^{(n-1)^2}$  of radius  $\sqrt{n-1}$ , centered at  $\mathbf{C}_n$ . This hypersphere is incident to the Birkhoff Polytope on the vertices.

**Proposition 1.** The gap as a ratio between  $\mathcal{DP}_n$  and both  $S^{(n-1)^2}$  and  $\mathcal{O}_n$  grows to infinity as  $n$  grows.

The proof is given in the supplementary document. While there exists polynomial time projections of the  $n!$ -element permutation space onto the continuous hypersphere representation and back [59], Prop. 1 prevents us from using hypersphere relaxations, as done in preceding works [59, 83].

## 4. Proposed Probabilistic Model

We assume that we are provided a set of pairwise, total permutations  $\mathbf{P}_{ij} \in \mathcal{P}_n$  for  $(i, j) \in \mathcal{E}$  and we are interested in finding the underlying *absolute permutations*  $\mathbf{X}_i$  for  $i \in \{1, \dots, N\}$  with respect to a common origin (e.g.  $\mathbf{X}_1 = \mathbf{I}$ , the identity matrix). We seek absolute permutations that would respect the consistency of the underlying graph structure. For conciseness, we also restrict our setting to total permutations, and leave the extension to partial permutations, which live on the *monoid*, as a future study. Because operating directly on  $\mathcal{P}_n$  would require us to solve a combinatorial optimization problem and because of the lack of a manifold structure for  $\mathcal{P}_n$ , we follow the popular approach [45, 80, 48] and relax the domain of the absolute permutations by assuming that each  $\mathbf{X}_i \in \mathcal{DP}_n$ .

We formulate the permutation synchronization problem in a probabilistic context where we treat the pairwise relative permutations as *observed* random variables and the absolute ones as *latent* random variables. In particular, our probabilistic construction enables us to cast the synchronization problem as inferential in the model. With a slight abuse of notation, in the rest of the paper, we will denote

$\mathbf{P} \equiv \{\mathbf{P}_{ij}\}_{(i,j) \in \mathcal{E}}$  and  $\mathbf{X} \equiv \{\mathbf{X}_i\}_{i=1}^N$ , all the observations and all the latent variables, respectively.

A typical way to build a probabilistic model is to first choose the prior distributions on  $\mathcal{DP}_n$  for each  $\mathbf{X}_i$  and then choose a conditional distribution on  $\mathcal{P}_n$  for each  $\mathbf{X}_{ij}$  given the latent variables. Unfortunately, standard parametric distributions neither exist on  $\mathcal{DP}_n$  nor on  $\mathcal{P}_n$ . The variational *stick breaking* [45] yields an *implicitly* defined PDF on  $\mathcal{DP}_n$  and is not able to provide direct control on the resulting distribution. Defining Kantorovich distance-based distributions over the permutation matrices is possible [17], yet these models incur high computational costs since they would require solving optimal transport problems during inference. For these reasons, instead of constructing a hierarchical probabilistic model, we will directly model the full joint distribution of  $\mathbf{P}$  and  $\mathbf{X}$ .

We propose a probabilistic model where we assume the full joint distribution admits the following factorized form:

$$p(\mathbf{P}, \mathbf{X}) = \frac{1}{Z} \prod_{(i,j) \in \mathcal{E}} \psi(\mathbf{P}_{ij}, \mathbf{X}_i, \mathbf{X}_j), \quad (8)$$

where  $Z$  denotes the normalization constant with

$$Z := \sum_{\mathbf{P} \in \mathcal{P}_n^{|\mathcal{E}|}} \int_{\mathcal{DP}_n^N} \prod_{(i,j) \in \mathcal{E}} \psi(\mathbf{P}_{ij}, \mathbf{X}_i, \mathbf{X}_j) d\mathbf{X}, \quad (9)$$

and  $\psi$  is called the ‘clique potential’ that is defined as:

$$\psi(\mathbf{P}_{ij}, \mathbf{X}_i, \mathbf{X}_j) \triangleq \exp(-\beta \|\mathbf{P}_{ij} - \mathbf{X}_i \mathbf{X}_j^\top\|_{\mathbb{F}}^2). \quad (10)$$

Here  $\|\cdot\|_{\mathbb{F}}$  denotes the Frobenius norm,  $\beta \in \mathbb{R}_+$  is the *dispersion* parameter that controls the spread of the distribution. Note that the model is a Markov random field [40].

Let us take a closer look at the proposed model. If we define  $\mathbf{X}_{ij} := \mathbf{X}_i \mathbf{X}_j^\top \in \mathcal{DP}_n$ , then by Thm. 1, we have the following decomposition for each  $\mathbf{X}_{ij}$ :

$$\mathbf{X}_{ij} = \sum_{b=1}^{B_{ij}} \theta_{ij,b} \mathbf{M}_{ij,b}, \quad \sum_{b=1}^{B_{ij}} \theta_{ij,b} = 1, \quad (11)$$

where  $B_{ij}$  is a positive integer, each  $\theta_{ij,b} \geq 0$ , and  $\mathbf{M}_{ij,b} \in \mathcal{P}_n$ . The next result states that we have an equivalent hierarchical interpretation for the proposed model:

**Proposition 2.** The probabilistic model defined in Eq. 8 implies the following hierarchical decomposition:

$$p(\mathbf{X}) = \frac{1}{C} \exp\left(-\beta \sum_{(i,j) \in \mathcal{E}} \|\mathbf{X}_{ij}\|^2\right) \prod_{(i,j) \in \mathcal{E}} Z_{ij} \quad (12)$$

$$p(\mathbf{P}_{ij} | \mathbf{X}_i, \mathbf{X}_j) = \frac{1}{Z_{ij}} \exp\left(2\beta \text{tr}(\mathbf{P}_{ij}^\top \mathbf{X}_{ij})\right) \quad (13)$$

where  $C$  and  $Z_{ij}$  are normalization constants. Besides, for all  $i, j$ ,  $Z_{ij} \geq \prod_{b=1}^{B_{ij}} f(\beta, \theta_{ij,b})$ , where  $f$  is a positive function that is increasing in both  $\beta$  and  $\theta_{ij,b}$ .

The proof is given in the supplementary and is based on the simple decomposition  $p(\mathbf{P}, \mathbf{X}) = p(\mathbf{X})p(\mathbf{P}|\mathbf{X})$ . This hierarchical point of view lets us observe some interesting properties: (1) the likelihood  $p(\mathbf{P}_{ij}|\mathbf{X}_i, \mathbf{X}_j)$  mainly depends on the term  $\text{tr}(\mathbf{P}_{ij}^\top \mathbf{X}_{ij})$  that measures the data fitness. We aptly call this term the ‘soft Hamming distance’ between  $\mathbf{P}_{ij}$  and  $\mathbf{X}_{ij}$  since it would correspond to the actual Hamming distance between two permutations if  $\mathbf{X}_i, \mathbf{X}_j$  were permutation matrices [41]. (2) On the other hand, the prior distribution contains two competing terms: (i) the term  $Z_{ij}$  favors large  $\theta_{ij,b}$ , which would push  $\mathbf{X}_{ij}$  towards the corners of the Birkhoff polytope, (ii) the term  $\|\mathbf{X}_{ij}\|_{\mathbb{F}}^2$  acts as a regularizer on the latent variables and attracts them towards the center of the Birkhoff polytope  $\mathbf{C}_n$  (cf. Dfn. 2), which will be numerically beneficial for the inference algorithms that will be developed in the following section.

## 5. Inference Algorithms

We can now formulate the permutation synchronization problem as a probabilistic inference problem, where we will be interested in the following quantities:

1. Maximum a-posteriori (MAP):

$$\mathbf{X}^* = \arg \max_{\mathbf{X} \in \mathcal{DP}_n^N} \log p(\mathbf{X}|\mathbf{P}) \quad (14)$$

where  $\log p(\mathbf{X}|\mathbf{P}) =^+ -\beta \sum_{(i,j) \in \mathcal{E}} \|\mathbf{P}_{ij} - \mathbf{X}_i \mathbf{X}_j^\top\|_{\mathbb{F}}^2$ , and  $=^+$  denotes equality up to an additive constant.

2. The full posterior distribution:  $p(\mathbf{X}|\mathbf{P}) \propto p(\mathbf{P}, \mathbf{X})$ .

The MAP estimate is often easier to obtain and useful in practice. On the other hand, characterizing the full posterior can provide important additional information, such as *uncertainty*; however, not surprisingly it is a much harder task. In addition to the usual difficulties associated with these tasks, in our context we are facing extra challenges due to the non-standard manifold of our latent variables.

### 5.1. Maximum A-Posteriori Estimation

The MAP estimation problem can be cast as a minimization problem on  $\mathcal{DP}_n$ , given as follows:

$$\mathbf{X}^* = \arg \min_{\mathbf{X} \in \mathcal{DP}_n^N} \left\{ U(\mathbf{X}) := \sum_{(i,j) \in \mathcal{E}} \|\mathbf{P}_{ij} - \mathbf{X}_i \mathbf{X}_j^\top\|_{\mathbb{F}}^2 \right\}$$

where  $U$  is called the potential energy function. We observe that the choice of the dispersion parameter has no effect on the MAP estimate. Although this optimization problem resembles conventional norm minimization, the fact that  $\mathbf{X}$  lives in the cartesian product of Birkhoff polytopes renders the problem very complicated.

Thanks to the retraction operator over the Birkhoff polytope (cf. Thm. 3), we are able to use several Riemannian optimization algorithms [69], without resorting to projection-based updates. In this study, we use the recently proposed

Riemannian limited-memory BFGS (LR-BFGS) [37], a powerful optimization technique that attains faster convergence rates by incorporating local geometric information in an efficient manner. This additional piece of information is obtained through an approximation of the inverse Hessian, which is computed on the most recent values of the past iterates with linear time- and space-complexity in the dimension of the problem. We give more detail on LR-BFGS in our supp. material. The detailed description of the algorithm can be found in [37, 82].

Finally, we round the resulting approximate solutions into a feasible one via Hungarian algorithm [52], obtaining binary permutation matrices.

### 5.2. Posterior Sampling via Riemannian Langevin Monte Carlo with Retractions

In this section we will develop a Markov Chain Monte Carlo (MCMC) algorithm for generating samples from the posterior distribution  $p(\mathbf{X}|\mathbf{P})$ , by borrowing ideas from [64, 46, 7]. Once such samples are generated, we will be able to quantify the uncertainty in our estimation by using the generated samples.

The dimension and complexity of the Birkhoff manifold makes it very challenging to generate samples on  $\mathcal{DP}_n$  or its product spaces and to the best of our knowledge there is no Riemannian MCMC algorithm that is capable of achieving this. There are existing Riemannian MCMC algorithms [11, 46], which are able to draw samples on embedded manifolds; however, they require the exact exponential map to be analytically available, which in our case, can only be approximated by the retraction map at best.

To this end, we develop an algorithmically simpler yet effective algorithm. Let the posterior density of interest be  $\pi_{\mathcal{H}}(\mathbf{X}) := p(\mathbf{X}|\mathbf{P}) \propto \exp(-\beta U(\mathbf{X}))$  with respect to the Hausdorff measure. We then define an *embedding*  $\xi : \mathbb{R}^{N(n-1)^2} \mapsto \mathcal{DP}_n^N$  such that  $\xi(\tilde{\mathbf{X}}) = \mathbf{X}$  for  $\tilde{\mathbf{X}} \in \mathbb{R}^{N(n-1)^2}$ . By the area formula (cf. Thm. 1 in [25]), we have the following expression for the embedded posterior density  $\pi_\lambda$  (with respect to the Lebesgue measure):

$$\pi_{\mathcal{H}}(\mathbf{x}) = \pi_\lambda(\tilde{\mathbf{X}}) / \sqrt{|\mathbf{G}(\tilde{\mathbf{X}})|}, \quad (15)$$

where  $\mathbf{G}$  denotes the Riemann metric tensor.

We then consider the following stochastic differential equation (SDE), which is a slight modification of the SDE that is used to develop the Riemannian Langevin Monte Carlo algorithm [31, 78, 58]:

$$d\tilde{\mathbf{X}}_t = (-\mathbf{G}^{-1} \nabla_{\tilde{\mathbf{X}}} U_\lambda(\tilde{\mathbf{X}}_t) + \mathbf{\Gamma}_t) dt + \sqrt{2/\beta \mathbf{G}^{-1}} dB_t,$$

where  $B_t$  denotes the standard Brownian motion and  $\mathbf{\Gamma}_t$  is called the correction term that is defined as follows:  $[\mathbf{\Gamma}_t(\tilde{\mathbf{X}})]_i = \sum_{j=1}^{N(n-1)^2} \partial[\mathbf{G}_t^{-1}(\tilde{\mathbf{X}})]_{ij} / \partial \tilde{\mathbf{X}}_j$ .

By Thm. 1 of [49], it is easy to show that the solution process  $(\tilde{\mathbf{X}}_t)_{t \geq 0}$  leaves the embedded posterior distribution



Figure 3. Sample images and manually annotated correspondences from the challenging Willow dataset [16]. Images are plotted in pairs (there are multiple) and in gray for better viewing.

$\pi_\lambda$  invariant. Informally, this result means that if we could exactly simulate the continuous-time process  $(\tilde{\mathbf{X}}_t)_{t \geq 0}$ , the distribution of the sample paths would converge to the embedded posterior distribution  $\pi_\lambda$ , and therefore the distribution of  $\xi(\tilde{\mathbf{X}}_t)$  would converge to  $\pi_{\mathcal{H}}(\mathbf{X})$ . However, unfortunately it is not possible to exactly simulate these paths and therefore we need to consult approximate algorithms.

A possible way to numerically simulate the SDE would be to use standard discretization tools, such as the Euler-Maruyama integrator [14]. However, this would require knowing the analytical expression of  $\xi$  and constructing  $\mathbf{G}_t$  and  $\mathbf{\Gamma}_t$  at each iteration. On the other hand, recent results have shown that we can simulate SDEs directly on their original manifolds by using geodesic integrators [11, 46, 34], which bypasses these issues altogether. Yet, these approaches require the exact exponential map of the manifold to be analytically available, restricting their applicability in our context.

Inspired by the recent manifold optimization algorithms [74], we propose to replace the exact, intractable exponential map arising in the geodesic integrator with the tractable retraction operator given in Thm. 3. We develop our recursive scheme, we coin as *retraction Euler integrator*:

$$\mathbf{V}_i^{(k+1)} = \Pi_{\mathbf{X}_i^{(k)}}(h\nabla_{\mathbf{X}_i} U(\mathbf{X}_i^{(k)}) + \sqrt{2h/\beta}\mathbf{Z}_i^{(k+1)}) \quad (16)$$

$$\mathbf{X}_i^{(k+1)} = R_{\mathbf{X}_i^{(k)}}(\mathbf{V}_i^{(k+1)}), \quad \forall i \in \{1, \dots, N\} \quad (17)$$

where  $h > 0$  denotes the step-size,  $k$  denotes the iterations,  $\mathbf{Z}_i^{(k)}$  denotes standard Gaussian random variables in  $\mathbb{R}^{n \times n}$ ,  $\mathbf{X}_i^{(0)}$  denotes the initial absolute permutations. The derivation of this scheme is similar to [46] and we provide more detailed information in the supplementary material. To the best of our knowledge, the convergence properties of the geodesic integrator that is approximated with a retraction operator have not yet been analyzed. We leave this analysis as a futurework, which is beyond the scope of this study.

We note that the term  $\|\mathbf{X}_{ij}\|_{\mathbb{F}}^2$  plays an important role in the overall algorithm since it prevents the latent variables  $\mathbf{X}_i$  to go the extreme points of the Birkhoff polytope, where the retraction operator becomes inaccurate. We also note that, when  $\beta \rightarrow \infty$ , the distribution  $\pi_{\mathcal{H}}$  concentrates on the global optimum  $\mathbf{X}^*$  and the proposed retraction Euler integrator becomes the Riemannian gradient descent with a retraction operator.

## 6. Experiments and Evaluations

### 6.1. Real Data

**2D Multi-image Matching** We run our method to perform multiway graph matching on two datasets, CMU [12] and Willow Object Class [16]. CMU is composed of House and Hotel objects viewed under constant illumination and smooth motion. Initial pairwise correspondences as well as ground truth (GT) absolute mappings are provided within the dataset. Object images in Willow dataset include pose, lighting, instance and environment variation as shown in Fig. 3, rendering naive template matching infeasible. For our evaluations, we follow the same design as Wang *et al.* [77]. We first extract local features from a set of  $227 \times 227$  patches centered around the annotated landmarks, using the prosperous Alexnet [42] pretrained on ImageNet [24]. Our descriptors correspond to the feature map responses of Conv4 and Conv5 layers anchored on the hand annotated keypoints. These features are then matched by the Hungarian algorithm [52] to obtain initial pairwise permutation matrices  $\mathbf{P}_0$ .

We initialize our algorithm by the closed form MatchEIG [51] and evaluate it against the state of the art methods of Spectral [56], MatchALS [85], MatchLift [36], MatchEIG [51], and Wang *et al.* [77]. The size of the universe is set to the number of features per image. We assume that this number is fixed and partial matches are not present. Handling partialities while using the Birkhoff structure is left as a future work. Note that [77] uses a similar cost function to ours in order to initialize an alternating procedure that in addition exploits the geometry of image coordinates. Authors also use this term as an extra bit of information during their initialization. The standard evaluation metric, *recall*, is defined over the pairwise permutations as:

$$R(\{\hat{\mathbf{P}}_i\}|\mathbf{P}^{\text{gnd}}) = \frac{1}{n|\mathcal{E}|} \sum_{(i,j) \in \mathcal{E}} \mathbf{P}_{ij}^{\text{gnd}} \odot (\hat{\mathbf{P}}_i \hat{\mathbf{P}}_j^\top) \quad (18)$$

where  $\mathbf{P}_{ij}^{\text{gnd}}$  are the GT relative transformations and  $\hat{\mathbf{P}}_i$  is an estimated permutation.  $R = 0$  in the case of no correctly found correspondences and  $R = 1$  for a perfect solution. Tab. 1 shows the results of different algorithms as well as ours. Note that our Birkhoff-LRBFSG method that operates solely on pairwise permutations outperforms all methods, even the ones which make use of geometry during initialization. Moreover, when our method is used to initialize Wang *et al.* [77] and perform geometric optimization, we attain the top results. These findings validate that walking on the Birkhoff Polytope, even approximately, and using Riemannian line-search algorithms constitute a promising direction for optimizing the problem at hand.

**Uncertainty Estimation in Real Data** We now run our confidence estimator on the same Willow Object Class [16].

Table 1. Our results on the *WILLOW Object Class* graph matching dataset.  $Wang^-$  refers to running Wang [77] without the geometric consistency term. The vanilla version of our method, *Ours*, already lacks this term. *Ours-Geom* then refers to initializing Wang’s verification method with our algorithm. For all the methods, we use the original implementation of the authors.

Dataset	Initial	Spectral [56]	MatchLift [36]	MatchALS [85]	MatchEig [51]	Wang <sup>-</sup> [77]	Ours	Wang [77]	Ours-Geom
Car	0.48	0.55	0.65	0.69	0.66	0.72	0.71	1.00	1.00
Duck	0.43	0.59	0.56	0.59	0.56	0.63	0.67	0.93 <sup>2</sup>	0.96
Face	0.86	0.92	0.94	0.93	0.93	0.95	0.95	1.00	1.00
Motorbike	0.30	0.25	0.27	0.34	0.28	0.40	0.37	1.00	1.00
Winebottle	0.52	0.64	0.72	0.70	0.71	0.73	0.73	1.00	1.00
CMU-House	0.68	0.90	0.94	0.92	0.94	0.98	0.98	1.00	1.00
CMU-Hotel	0.64	0.81	0.87	0.86	0.92	0.94	0.96	1.00	1.00
Average	0.52	0.59	0.65	0.66	0.71	0.76	<b>0.77</b>	0.99	<b>0.99</b>

To do that, we first find the optimal point where synchronization is at its best. Then, we set  $h \leftarrow 0.0001$ ,  $\beta \leftarrow [0.075, 0.1]$  and automatically start sampling the posterior around this mode for 1000 iterations. Note that  $\beta$  is a critical parameter which can also be dynamically controlled [7]. Larger values of  $\beta$  cannot provide enough variation for a good diversity of solutions. Smaller values cause greater random perturbations leading to samples far from the optimum. This can cause divergence or samples not explaining the local mode. Nevertheless, all our tests worked well with values in the given range.

The generated samples are useful in many applications, e.g. fitting distributions or providing additional solution hints. We address the case of multiple hypotheses generation for the permutation synchronization problem and show that generating an additional per-edge candidate with high certainty helps to improve the recall. Tab. 2 shows the top-K scores we achieve by simply incorporating  $K$  likely samples. Note that, when 2 matches are drawn at random and contribute as potentially correct matches, the recall is increased only by 2%, whereas including our samples instead boosts the multi-way matching by 6%.

Table 2. Using **top-K** errors to rank by uncertainty. Based on the confidence information we could retain multiple hypotheses. This is not possible by the other approaches such as Wang *et al.* [51, 77]. *Rand-K* refers to using  $K - 1$  additional random hypotheses to complement the found solution. *Ours-K* ranks assignments by our probabilistic certainty and retains top-K candidates per point.

Dataset	Wang	Ours	Rand-2	Ours-2	Rand-3	Ours-3
Car	0.72	0.71	0.73	0.76	0.76	0.81
Duck	0.63	0.67	0.67	0.69	0.67	0.72
Face	0.95	0.95	0.96	0.97	0.96	0.98
Motorbike	0.40	0.37	0.45	0.49	0.52	0.60
Winebottle	0.73	0.74	0.77	0.82	0.79	0.85
Avg.	0.69	0.69	0.71	<b>0.75</b>	0.74	<b>0.79</b>

We further present illustrative results for our confidence prediction in Fig. 4. There, unsatisfactory solutions arising in certain cases are improved by analyzing the uncertainty

<sup>2</sup> [77] reports a value of 0.88, but for their method, we attained 0.93 and therefore report this value.

map. The column (e) of the figure depicts the top-2 assignments retained in the confidence map and (e) plots the assignments that overlap with the true solution. Note that, we might not have access to such an oracle in real applications and only show this to illustrate potential use cases of the estimated confidence map.

## 6.2. Evaluations on Synthetic Data

We synthetically generate 28 different problems with varying sizes:  $M \in [10, 100]$  nodes and  $n \in [16, 100]$  points in each node. For the scenario of image matching, this would correspond to  $M$  cameras and  $N$  features in each image. We then introduce 15% – 35% random swaps to the GT absolute permutations and compute the *observed* relative ones. Details of this dataset are given in suppl. material. Among all 28 sets of synthetic data, we attain an overall recall of 91% whereas MatchEIG [51] remains about 83%.

**Runtime Analysis** Next, we assess the computational cost of our algorithm against the state of the art methods, on the dataset explained above. All of our experiments are run on a MacBook computer with an Intel i7 2.8GhZ CPU. Our implementation uses a modified Ceres solver [1]. All the other algorithms use highly vectorized MATLAB 2017b code making our comparisons reasonably fair. Fig. 5 tabulates runtimes for different methods excluding initialization. *MatchLift* easily took more than 20min. for moderate problems and hence we choose to exclude it from this evaluation. It is noticeable that thanks to the ability of using more advanced solvers such as LBFGS, our method converges much faster than Wang *et al.* and runs on par with the fastest yet least accurate spectral synchronization [56]. The worst case theoretical computational complexity of our algorithm is  $O_{B-LRBFGS} := O(K|\mathcal{E}|K_S(n^2 + (2n)^3))$  where  $K$  is the number of LBFGS iterations and  $K_S$  the number of Sinkhorn iterations. While  $K_S$  can be a bottleneck, in practice our matrices are already restricted to the Birkhoff manifold and Sinkhorn early-terminates, letting  $K_S$  remain small. The complexity is: (1) linearly-dependent upon the number of edges, which in the worst case relates quadratically to the number of images  $|\mathcal{E}| = N(N-1)$ , (2) cubically dependent on  $n$ . This is due to the fact that projection onto

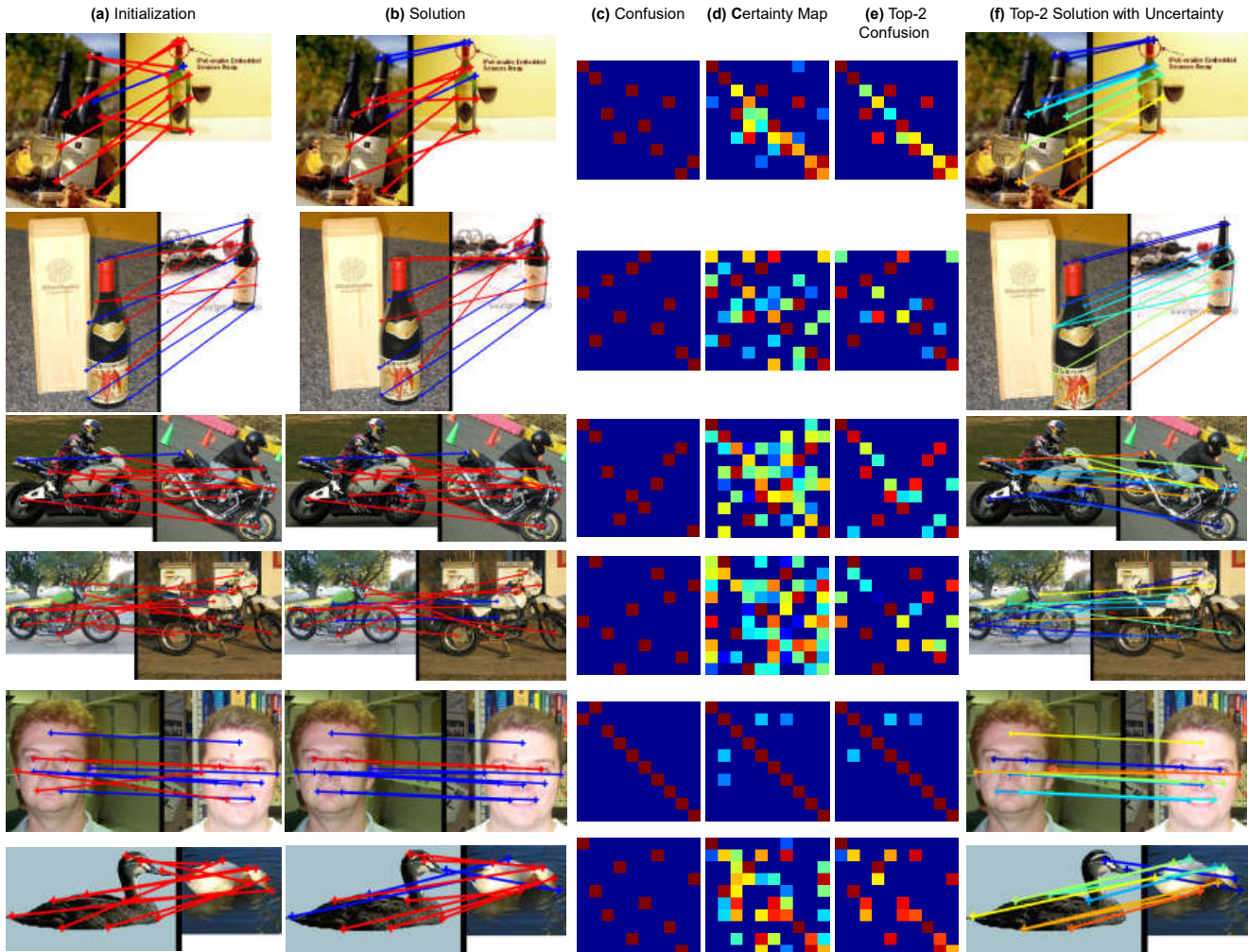


Figure 4. Results from our confidence estimation. Given potentially erroneous solutions (b) to the problems initialized as in (a), our latent samples discover the uncertain assignments as shown in the middle three columns (c-e). When multiple top-2 solutions are accepted as potential positives, our method can suggest high quality hypotheses (f). The edges in the last column (f) is colored by their confidence value. Note that even though, for the sake of space we show pairs of images, the datasets contain multiple sets of images.

the tangent space solves a system of  $2n \times 2n$  equations.

## 7. Conclusion

In this work we have proposed two new frameworks for relaxed permutation synchronization on the manifold of doubly stochastic matrices. Our novel model and formulation paved the way to using sophisticated optimizers such as Riemannian limited-memory BFGS. We further integrated a manifold-MCMC scheme enabling posterior sampling and thereby confidence estimation. We have shown that our confidence maps are informative about cycle inconsistencies and can lead to new solution hypotheses. We used these hypotheses in a top-K evaluation and illustrated its benefits. In the future, we plan to (i) address partial permutations, the inner region of the Birkhoff Polytope (ii) investigate more sophisticated MCMC schemes such as [28, 34, 63, 46, 65]

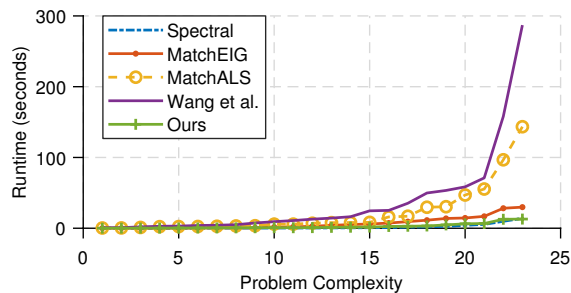


Figure 5. Running times of different methods with increasing problem size:  $N \in [10, 100]$  and  $n \in [16, 100]$ .

(iii) seek better use cases for our confidence estimates such as outlier removal.

**Acknowledgements:** Supported by the grant ANR-16-CE23-0014 (FBI-MATRIX). Authors thank Haowen Deng for the initial 3D correspondences and, Benjamin Busam and Jesus Briaes for fruitful discussions.

## References

- [1] Sameer Agarwal, Keir Mierle, and Others. Ceres solver. <http://ceres-solver.org>.
- [2] Federica Arrigoni, Eleonora Maset, and Andrea Fusiello. Synchronization in the symmetric inverse semigroup. In *International Conference on Image Analysis and Processing*, pages 70–81. Springer, 2017.
- [3] Federica Arrigoni, Beatrice Rossi, and Andrea Fusiello. Spectral synchronization of multiple views in se (3). *SIAM Journal on Imaging Sciences*, 9(4):1963–1990, 2016.
- [4] Florian Bernard, Johan Thunberg, Peter Gemmar, Frank Hertel, Andreas Husch, and Jorge Goncalves. A solution for multi-alignment by transformation synchronisation. In *Proceedings of the IEEE Conference on Computer Vision and Pattern Recognition*, pages 2161–2169, 2015.
- [5] Florian Bernard, Johan Thunberg, Jorge Goncalves, and Christian Theobalt. Synchronisation of partial multi-matchings via non-negative factorisations. *CoRR*, abs/1803.06320, 2018.
- [6] Tolga Birdal, Emrah Bala, Tolga Eren, and Slobodan Ilic. Online inspection of 3d parts via a locally overlapping camera network. In *2016 IEEE Winter Conference on Applications of Computer Vision (WACV)*, pages 1–10. IEEE, 2016.
- [7] Tolga Birdal, Umut Şimşekli, M. Onur Eken, and Slobodan Ilic. Bayesian Pose Graph Optimization via Bingham Distributions and Tempered Geodesic MCMC. In *Advances in Neural Information Processing Systems (NeurIPS)*, 2018.
- [8] Tolga Birdal and Slobodan Ilic. Cad priors for accurate and flexible instance reconstruction. In *Proceedings of the IEEE International Conference on Computer Vision*, 2017.
- [9] Garrett Birkhoff. Tres observaciones sobre el algebra lineal. *Univ. Nac. Tucumán Rev. Ser. A*, 5:147–151, 1946.
- [10] Benjamin Busam, Marco Esposito, Simon Che’Rose, Nassir Navab, and Benjamin Frisch. A stereo vision approach for cooperative robotic movement therapy. In *IEEE International Conference on Computer Vision Workshop (ICCVW)*, December 2015.
- [11] Simon Byrne and Mark Girolami. Geodesic monte carlo on embedded manifolds. *Scandinavian Journal of Statistics*, 40(4):825–845, 2013.
- [12] Tibério S Caetano, Julian J McAuley, Li Cheng, Quoc V Le, and Alex J Smola. Learning graph matching. *IEEE transactions on pattern analysis and machine intelligence*, 31(6):1048–1058, 2009.
- [13] Kunal N Chaudhury, Yuehaw Khoo, and Amit Singer. Global registration of multiple point clouds using semidefinite programming. *SIAM Journal on Optimization*, 25(1):468–501, 2015.
- [14] Changyou Chen, Nan Ding, and Lawrence Carin. On the convergence of stochastic gradient MCMC algorithms with high-order integrators. In *Advances in Neural Information Processing Systems*, pages 2278–2286, 2015.
- [15] Yuxin Chen, Leonidas Guibas, and Qixing Huang. Near-optimal joint object matching via convex relaxation. In *Proceedings of the 31st International Conference on International Conference on Machine Learning - Volume 32, ICML’14*, pages II–100–II–108. JMLR.org, 2014.
- [16] Minsu Cho, Karteek Alahari, and Jean Ponce. Learning graphs to match. In *Proceedings of the IEEE International Conference on Computer Vision*, pages 25–32, 2013.
- [17] Stéphan Cléménçon and Jérémie Jakubowicz. Kantorovich distances between rankings with applications to rank aggregation. In *Joint European Conference on Machine Learning and Knowledge Discovery in Databases*. Springer, 2010.
- [18] Luca Cosmo, Andrea Albarelli, Filippo Bergamasco, Andrea Torsello, Emanuele Rodolà, and Daniel Cremers. A game-theoretical approach for joint matching of multiple feature throughout unordered images. In *Pattern Recognition (ICPR), 2016 23rd International Conference on*, pages 3715–3720. IEEE, 2016.
- [19] Luca Cosmo, Emanuele Rodolà, Andrea Albarelli, Facundo Mémoli, and Daniel Cremers. Consistent partial matching of shape collections via sparse modeling. In *Computer Graphics Forum*, volume 36, pages 209–221. Wiley Online Library, 2017.
- [20] Angela Dai, Matthias Nießner, Michael Zollhöfer, Shahram Izadi, and Christian Theobalt. Bundlefusion: Real-time globally consistent 3d reconstruction using on-the-fly surface reintegration. *ACM Transactions on Graphics (TOG)*, 36(4):76a, 2017.
- [21] Joseph DeGol, Timothy Bretl, and Derek Hoiem. Improved structure from motion using fiducial marker matching. In *Proceedings of the European Conference on Computer Vision (ECCV)*, pages 273–288, 2018.
- [22] Haowen Deng, Tolga Birdal, and Slobodan Ilic. Ppf-foldnet: Unsupervised learning of rotation invariant 3d local descriptors. In *Proceedings of the European Conference on Computer Vision (ECCV)*, pages 602–618, 2018.
- [23] Haowen Deng, Tolga Birdal, and Slobodan Ilic. Ppfnet: Global context aware local features for robust

- 3d point matching. In *The IEEE Conference on Computer Vision and Pattern Recognition (CVPR)*, June 2018.
- [24] Jia Deng, Wei Dong, Richard Socher, Li-Jia Li, Kai Li, and Li Fei-Fei. Imagenet: A large-scale hierarchical image database. In *IEEE Conference on Computer Vision and Pattern Recognition*. Ieee, 2009.
- [25] Persi Diaconis, Susan Holmes, Mehrdad Shahshahani, et al. Sampling from a manifold. In *Advances in Modern Statistical Theory and Applications: A Festschrift in honor of Morris L. Eaton*. Institute of Mathematical Statistics, 2013.
- [26] A. Douik and B. Hassibi. Manifold Optimization Over the Set of Doubly Stochastic Matrices: A Second-Order Geometry. *ArXiv e-prints*, Feb. 2018.
- [27] Fanny Dufossé, Kamer Kaya, Ioannis Panagiotas, and Bora Uçar. *Further notes on Birkhoff-von Neumann decomposition of doubly stochastic matrices*. PhD thesis, Inria-Research Centre Grenoble–Rhône-Alpes, 2017.
- [28] Alain Durmus, Umut Simsekli, Eric Moulines, Roland Badeau, and Gaël Richard. Stochastic gradient Richardson-Romberg Markov Chain Monte Carlo. In *Advances in Neural Information Processing Systems*, pages 2047–2055, 2016.
- [29] Rizal Fathony, Sima Behpour, Xinhua Zhang, and Brian Ziebart. Efficient and consistent adversarial bipartite matching. In *International Conference on Machine Learning*, pages 1456–1465, 2018.
- [30] P. Gargallo. Using opensfm. Online. Accessed May-2018.
- [31] Mark Girolami and Ben Calderhead. Riemann manifold Langevin and Hamiltonian Monte Carlo methods. *Journal of the Royal Statistical Society: Series B 118 (Statistical Methodology)*, 73(2):123–214, 2011.
- [32] Michel X Goemans. Smallest compact formulation for the permutahedron. *Mathematical Programming*, 2015.
- [33] Venu Madhav Govindu. Lie-algebraic averaging for globally consistent motion estimation. In *Proceedings of the 2004 IEEE Computer Society Conference on Computer Vision and Pattern Recognition, 2004. CVPR 2004.*, volume 1, pages I–I. IEEE, 2004.
- [34] Andrew Holbrook. Note on the geodesic monte carlo. *arXiv preprint arXiv:1805.05289*, 2018.
- [35] Nan Hu, Qixing Huang, Boris Thibert, UG Alpes, and Leonidas Guibas. Distributable consistent multi-object matching. In *Proceedings of the IEEE Conference on Computer Vision and Pattern Recognition*, 2018.
- [36] Qi-Xing Huang and Leonidas Guibas. Consistent shape maps via semidefinite programming. In *Proceedings of the Eleventh Eurographics/ACMSIGGRAPH Symposium on Geometry Processing*. Eurographics Association, 2013.
- [37] Wen Huang, Kyle A Gallivan, and P-A Absil. A broyden class of quasi-newton methods for riemannian optimization. *SIAM Journal on Optimization*, 25(3):1660–1685, 2015.
- [38] Daniel F Huber and Martial Hebert. Fully automatic registration of multiple 3d data sets. *Image and Vision Computing*, 21(7):637–650, 2003.
- [39] GLENN Hurlbert. A short proof of the birkhoff-von neumann theorem. *preprint (unpublished)*, 2008.
- [40] Ross Kindermann. Markov random fields and their applications. *American mathematical society*, 1980.
- [41] Anna Korba, Alexandre Garcia, and Florence d’Alché Buc. A structured prediction approach for label ranking. *arXiv preprint arXiv:1807.02374*, 2018.
- [42] Alex Krizhevsky, Ilya Sutskever, and Geoffrey E Hinton. Imagenet classification with deep convolutional neural networks. In *Advances in neural information processing systems*, pages 1097–1105, 2012.
- [43] Hongdong Li and Richard Hartley. The 3d-3d registration problem revisited. In *Computer Vision, 2007. ICCV 2007. IEEE 11th International Conference on*, pages 1–8. IEEE, 2007.
- [44] Xinchao Li, Martha Larson, and Alan Hanjalic. Pairwise geometric matching for large-scale object retrieval. In *Proceedings of the IEEE Conference on Computer Vision and Pattern Recognition*, pages 5153–5161, 2015.
- [45] Scott Linderman, Gonzalo Mena, Hal Cooper, Liam Paninski, and John Cunningham. Reparameterizing the birkhoff polytope for variational permutation inference. In *International Conference on Artificial Intelligence and Statistics*, pages 1618–1627, 2018.
- [46] Chang Liu, Jun Zhu, and Yang Song. Stochastic gradient geodesic mcmc methods. In *Advances in Neural Information Processing Systems*, pages 3009–3017, 2016.
- [47] David G Lowe. Distinctive image features from scale-invariant keypoints. *International journal of computer vision*, 60(2):91–110, 2004.
- [48] Vince Lyzinski, Donniell E Fishkind, Marcelo Fiori, Joshua T Vogelstein, Carey E Priebe, and Guillermo Sapiro. Graph matching: Relax at your own risk. *IEEE transactions on pattern analysis and machine intelligence*, 38(1):60–73, 2016.
- [49] Yi-An Ma, Tianqi Chen, and Emily Fox. A complete recipe for stochastic gradient MCMC. In *Advances in*

- Neural Information Processing Systems*, pages 2917–2925, 2015.
- [50] João Maciel and João Paulo Costeira. A global solution to sparse correspondence problems. *IEEE Transactions on Pattern Analysis and Machine Intelligence*, 25(2), 2003.
- [51] E. Maset, F. Arrigoni, and A. Fusiello. Practical and efficient multi-view matching. In *2017 IEEE International Conference on Computer Vision (ICCV)*, Oct 2017.
- [52] James Munkres. Algorithms for the assignment and transportation problems. *Journal of the society for industrial and applied mathematics*, 5(1):32–38, 1957.
- [53] Raúl Mur-Artal and Juan D. Tardós. ORB-SLAM2: an open-source SLAM system for monocular, stereo and RGB-D cameras. *IEEE Transactions on Robotics*, 33(5):1255–1262, 2017.
- [54] Andy Nguyen, Mirela Ben-Chen, Katarzyna Welnicka, Yinyu Ye, and Leonidas Guibas. An optimization approach to improving collections of shape maps. In *Computer Graphics Forum*, volume 30, pages 1481–1491. Wiley Online Library, 2011.
- [55] Deepti Pachauri, Risi Kondor, Gautam Sargur, and Vikas Singh. Permutation diffusion maps (pdm) with application to the image association problem in computer vision. In *Advances in Neural Information Processing Systems*, pages 541–549, 2014.
- [56] Deepti Pachauri, Risi Kondor, and Vikas Singh. Solving the multi-way matching problem by permutation synchronization. In *Advances in neural information processing systems*, pages 1860–1868, 2013.
- [57] Han-Mu Park and Kuk-Jin Yoon. Consistent multiple graph matching with multi-layer random walks synchronization. *Pattern Recognition Letters*, 2018.
- [58] Sam Patterson and Yee Whye Teh. Stochastic gradient Riemannian Langevin dynamics on the probability simplex. In *Advances in Neural Information Processing Systems*, pages 3102–3110, 2013.
- [59] Sergey Plis, Stephen McCracken, Terran Lane, and Vince Calhoun. Directional statistics on permutations. In *Proceedings of the Fourteenth International Conference on Artificial Intelligence and Statistics*, pages 600–608, 2011.
- [60] Torsten Sattler, Tobias Weyand, Bastian Leibe, and Leif Kobbelt. Image retrieval for image-based localization revisited, 2012.
- [61] Michele Schiavinato and Andrea Torsello. Synchronization over the birkhoff polytope for multi-graph matching. In *International Workshop on Graph-Based Representations in Pattern Recognition*, pages 266–275. Springer, 2017.
- [62] Johannes L Schonberger and Jan-Michael Frahm. Structure-from-motion revisited. In *Proceedings of the IEEE Conference on Computer Vision and Pattern Recognition*, pages 4104–4113, 2016.
- [63] Umut Şimşekli. Fractional Langevin Monte Carlo: Exploring Lévy driven stochastic differential equations for Markov Chain Monte Carlo. In *International Conference on Machine Learning*, pages 3200–3209. JMLR. org, 2017.
- [64] Umut Simsekli, Roland Badeau, Taylan Cemgil, and Gaël Richard. Stochastic quasi-Newton Langevin Monte Carlo. In *International Conference on Machine Learning (ICML)*, 2016.
- [65] Umut Şimşekli, Çağatay Yıldız, Thanh Huy Nguyen, Gaël Richard, and A Taylan Cemgil. Asynchronous stochastic quasi-Newton MCMC for non-convex optimization. In *International Conference on Machine Learning*, 2018.
- [66] Amit Singer. Angular synchronization by eigenvectors and semidefinite programming. *Applied and computational harmonic analysis*, 30(1):20, 2011.
- [67] Amit Singer and Yoel Shkolnisky. Three-dimensional structure determination from common lines in cryo-em by eigenvectors and semidefinite programming. *SIAM journal on imaging sciences*, 4(2):543–572, 2011.
- [68] Richard Sinkhorn and Paul Knopp. Concerning non-negative matrices and doubly stochastic matrices. *Pacific Journal of Mathematics*, 21(2):343–348, 1967.
- [69] Steven T Smith. Optimization techniques on Riemannian manifolds. *Fields institute communications*, 3(3):113–135, 1994.
- [70] Yifan Sun, Zhenxiao Liang, Xiangru Huang, and Qixing Huang. Joint map and symmetry synchronization. In *Proceedings of the European Conference on Computer Vision (ECCV)*, pages 251–264, 2018.
- [71] Da Tang and Tony Jebara. Initialization and coordinate optimization for multi-way matching. In *Artificial Intelligence and Statistics*, pages 1385–1393, 2017.
- [72] Johan Thunberg, Florian Bernard, and Jorge Goncalves. Distributed methods for synchronization of orthogonal matrices over graphs. *Automatica*, 80:243–252, 2017.
- [73] Bill Triggs, Philip F McLauchlan, Richard I Hartley, and Andrew W Fitzgibbon. Bundle adjustment—a modern synthesis. In *International workshop on vision algorithms*, pages 298–372. Springer, 1999.
- [74] Nilesh Tripuraneni, Nicolas Flammarion, Francis Bach, and Michael I Jordan. Averaging stochastic gradient descent on Riemannian manifolds. In *Conference on Learning Theory (COLT)*, 2018.

- [75] Roberto Tron and Rene Vidal. Distributed 3-d localization of camera sensor networks from 2-d image measurements. *IEEE Transactions on Automatic Control*, 59(12):3325–3340, 2014.
- [76] Lanhui Wang and Amit Singer. Exact and stable recovery of rotations for robust synchronization. *Information and Inference: A Journal of the IMA*, 2(2):145–193, 2013.
- [77] Qianqian Wang, Xiaowei Zhou, and Kostas Daniilidis. Multi-image semantic matching by mining consistent features. In *CVPR*, 2018.
- [78] Tatiana Xifara, Chris Sherlock, Samuel Livingstone, Simon Byrne, and Mark Girolami. Langevin diffusions and the Metropolis-adjusted Langevin algorithm. *Statistics & Probability Letters*, 91:14–19, 2014.
- [79] Junchi Yan, Minsu Cho, Hongyuan Zha, Xiaokang Yang, and Stephen M Chu. Multi-graph matching via affinity optimization with graduated consistency regularization. *IEEE transactions on pattern analysis and machine intelligence*, 38(6):1228–1242, 2016.
- [80] Junchi Yan, Xu-Cheng Yin, Weiyao Lin, Cheng Deng, Hongyuan Zha, and Xiaokang Yang. A short survey of recent advances in graph matching. In *Proceedings of the 2016 ACM on International Conference on Multimedia Retrieval*, pages 167–174. ACM, 2016.
- [81] Jin-Gang Yu, Gui-Song Xia, Ashok Samal, and Jinwen Tian. Globally consistent correspondence of multiple feature sets using proximal gauss–seidel relaxation. *Pattern Recognition*, 51:255–267, 2016.
- [82] Xinru Yuan, Wen Huang, P-A Absil, and Kyle A Gallivan. A riemannian limited-memory BFGS algorithm for computing the matrix geometric mean. *Procedia Computer Science*, 80:2147–2157, 2016.
- [83] Andrei Zanfir and Cristian Sminchisescu. Deep learning of graph matching. In *The IEEE Conference on Computer Vision and Pattern Recognition (CVPR)*, June 2018.
- [84] Mikhail Zaslavskiy, Francis Bach, and Jean-Philippe Vert. A path following algorithm for the graph matching problem. *IEEE Transactions on Pattern Analysis and Machine Intelligence*, 31(12):2227–2242, 2009.
- [85] Xiaowei Zhou, Menglong Zhu, and Kostas Daniilidis. Multi-image matching via fast alternating minimization. In *Proceedings of the IEEE International Conference on Computer Vision*, pages 4032–4040, 2015.